Available online at www.sciencedirect.com
ScienceDirect
International Journal of Mass Spectrometry 257 (2006) 60–69
International Journal of Mass Spectrometry
www.elsevier.com/locate/ijms

Gas phase reactivity of Cu^+-aromatic amino acids An experimental and theoretical study

A. Rimola [a], M. Sodupe [a], J. Tortajada [b], L. Rodríguez-Santiago [a,*]

[a] *Departament de Química, Universitat Autònoma de Barcelona, Bellaterra 08193, Spain*
[b] *Laboratoire Analyse et Modélisation pour la Biologie et l'Environnement, CNRS UMR 8587, Université d'Evry-Val-d'Essonne, Bât. Maupertuis, Boulevard François Mitterrand 91025 Evry Cedex, Spain*

Received 19 May 2006; received in revised form 21 June 2006; accepted 22 June 2006
Available online 25 July 2006

Abstract

The reactions between Cu^+ and the four natural aromatic amino acids (AA_{arom} = Phe, Tyr, Trp and His) have been investigated by means of electrospray ionization mass spectrometry. Metal cation complexes ([Cu AA_{arom}]$^+$) were formed in the electrospray source and collision-induced fragmentations of the most abundant isotopic form, [^{63}Cu AA_{arom}]$^+$, were studied for each amino acid. The same fragmentation pattern is observed for all the amino acids, the most important peak corresponding in all cases to the loss of CH_2O_2. Among the four aromatic amino acids, the [Cu Phe]$^+$ complex was selected for a computational study of the potential energy surface. Several mechanisms were studied at the B3LYP level and most of the observed fragmentations start with the metal cation insertion into the C–C backbone bond or into the C–R bond of the amino acid.

Keywords: Metal cation; Aromatic amino acids; ESI-CID; B3lyp

1. Introduction

During the past years, considerable attention has been directed towards the properties of gas phase complexes between bare transition metal cations and relevant biological molecules [1–3] particularly because metal cations interaction with neutral compounds implies a reorganization of the charge density of the neutral moiety, which leads to an activation of some particular bonds that affects reactivity [4–6]. Furthermore, gas phase studies of transition metals interaction with biomolecules enable us to know their intrinsic properties and can provide important clues to understand the behaviour of more complicated systems of biological importance.

Mass spectrometry techniques are very valuable for the study of the interactions of metal cation–biomolecule complexes in gas phase. Particularly, in the last years, the development of electrospray ionization (ESI) and matrix-assisted laser desorption–ionization (MALDI) has generalized the use of mass spectrometry in the study of these systems. Mass spectrometry permits not only to determine binding energies, but also to study the reactivity induced by the activated bonds as a consequence of the ion–neutral interaction. For example, the analysis of the fragmentations of metal cationized peptides produced under mass spectrometry conditions can provide complementary information for peptide sequencing when the fragmentation of the protonated peptide is not enough [7–11]. Moreover, the spontaneous fragmentations or collision-induced dissociation processes (CID) of the ion–neutral complexes observed can also provide information on the bonding and on some features of their potential energy surface (PES).

There are 20 natural amino acids, among which 4 have an aromatic chain: histidine (*His*), phenylalanine (*Phe*), tyrosine (*Tyr*) and tryptophane (*Trp*). The aromatic group enable these amino acids to establish an additional interaction with metal cations: cation–π interactions [12]. These kind of interactions are non-covalent binding forces which involve the π-face of the aromatic amino acid, and are very important in many biochemical processes such as biological molecular recognition and enzyme catalysis [12,13]. In the case of *His* the complexity is increased because its acid–basic chain confers several additional protonation and coordination sites [14,15]. It is well known that in some biological processes *His* residues are often involved in the active sites interacting with metal cations [16].

* Corresponding author. Tel.: +34 93 581 1671; fax: +34 93 581 2920.
E-mail address: luis@qf.uab.es (L. Rodríguez-Santiago).

1387-3806/$ – see front matter © 2006 Elsevier B.V. All rights reserved.
doi:10.1016/j.ijms.2006.06.017

The interaction of different metal cations with amino acids, including the aromatic ones, have been studied by several authors from an experimental point of view, with special emphasis on copper ions [17–27]. Since they play an important role in several biological processes such as electron transfer or dioxygen transport [28] Harrison and co-workers have reported the fragmentation reactions of several Cu^+ cationized amino acids generated by fast atom bombardment (FAB) [18]. Lavanant and Hoppilliard [19] have studied the formation and fragmentation of α-amino acids complexed by Cu^+ in plasma desorption mass spectrometry (PDMS). It is proposed that the fragmentations of the complexes generated are induced by an insertion of the metal cation into the amino acid bonds. For all these fragmentations, the loss of mass 46 is mostly observed under CID conditions. This loss is also observed by different mass spectrometry techniques with other metal cations such as Ni^+ and Fe^+ [21,29–31]. Theoretical calculations suggest that this mass of 46 u is associated to the losses of H_2O and CO [27,30].

On the other hand, reactions of Ag^+ with *Phe* have also been studied both from experimental and theoretical points of view [32,33]. The fragmentation spectra obtained by ESI–CID showed several peaks, the most relevant ones being those corresponding to the loss of H_2O followed by CO, the loss of NH_3 and CO, and the simultaneous loss of NH_3 and CO_2. They also observed the formation and the loss of AgH, and a peak belonging to the $[Ag\ NH_3]^+$ complex.

The interaction of Cu^+, a closed shell cation with a d^{10} (^1S) ground state, with formamide, guanidine, glycine, urea, and other molecules that can be taken as model of biochemical systems has been investigated theoretically in our groups [34–37]. In the last years, theoretical calculations have been used to rationalize the fragmentation processes of the complexes generated by mass spectrometry by analyzing different reaction mechanisms. Recently, Hoppilliard et al. have presented an exhaustive theoretical study of the fragmentation mechanisms of the complexes of Cu^+ with glycine ($[Cu\ Gly]^+$) generated by ESI-MS [27].

In the present work, we will show the results, from an electrosprayed solution, of Cu^+ with the four natural aromatic amino acids jointly with the fragmentations observed in the collision cell of a triple quadrupole mass spectrometer. With the aim of proposing an interpretation of the low energy decomposition processes for $[Cu\ AA_{arom}]^+$ systems, the fragmentation mechanisms have been investigated by means of density functional calculations only for $[Cu\ Phe]^+$ as a model system. Thus, we have theoretically studied the possible modes of coordination of Cu^+ to *Phe* along with the possible pathways of decomposition that lead to the experimentally observed fragments.

2. Experimental

Electrospray mass spectra were recorded on an Applied Biosystems/MDS Sciex API2000 triple-quadrupole instrument fitted with a "turboionspray" ion source. Samples were introduced in the source using direct infusion with a syringe pump, at a flow rate of 8 μl/min. Ionization of the samples was achieved by applying a voltage of 5.0 kV on the sprayer probe and by the use of a nebulizing gas (GAS1, air) surrounding the sprayer probe, intersected by a heated gas (GAS2, air) at an angle of approximately 90°. The operating pressure of GAS1 and GAS2 are adjusted to 2.0 bar, by means of an electronic board (pressure sensors), as a fraction of the air inlet pressure. The curtain gas (N_2), which prevents air or solvent from entering the analyzer region, was similarly adjusted to a value of 2.0 bar. The temperature of GAS2 was set to 70 °C. MS/MS spectra were carried out by introducing nitrogen as collision gas in the second quadrupole at a total pressure of 3×10^{-5} mbar, the background pressure being around 10^{-5} mbar. As detailed later, the declustering potential (DP), defined as the difference of potentials between the orifice plate and the skimmer (grounded), and typically referred to as the "cone voltage" for other electrospray interfaces, was fixed to 100 V to perform MS/MS experiments (110 V in case of *Phe*).

Unless otherwise noted, mass to charge ratios mentioned in throughout this paper refer to as peaks which include the most abundant Cu isotope (^{63}Cu).

Amino acids and copper salts were purchased from Aldrich and were used without further purification. Sample solutions were prepared from $CuSO_4{\cdot}5H_2O$/amino acid mixture with concentrations of 10^{-4} mol L^{-1} in a methanol/water 1:1 solvent.

3. Computational details

Molecular geometries and harmonic vibrational frequencies of the considered structures have been obtained using the non-local hybrid three-parameter B3LYP [38,39] density functional approach, as implemented in Gaussian 03 set of programs package [40]. In some cases we have carried out intrinsic reaction coordinate (IRC) calculations at the same level of theory in order to corroborate the minima connected by a given transition state. Previous theoretical calculations have shown that B3LYP approach is a cost-effective method for studying transition metal cation–ligand systems, yielding binding energies in fairly good agreement with the experimental values [41–43]. However, in order to assess the reliability of the calculate B3LYP energies for this $[Cu\ AA]^+$ systems, the CCSD(T) binding energy for the most stable structure of $[Cu\ Phe]^+$ has also been computed, the difference between both methods being only 0.6 kcal/mol (the value of D_0 is 83.5 kcal/mol at the B3LYP level and 82.9 at the CCSD(T) one).

Geometry optimizations and frequency calculations have been performed using the following basis set. For Cu we employed the Watchers' primitive set (14s9p5d), [44] supplemented with one s, two p and one d diffuse functions [44,45] and one f polarization function [46]. The final basis set is of the form (15s11p6d1f)/[10s7p4d1f]. For C, N, O and H we have used the 6-31++G(d,p) basis set.

4. Results and discussion

The electrospray spectra of the copper sulfate/amino acid mixtures is dependent on the cone voltage, also referred to as declustering potential (DP) in our instrument. At all low values of DP the spectra are dominated by different Cu^+ and Cu^{2+}

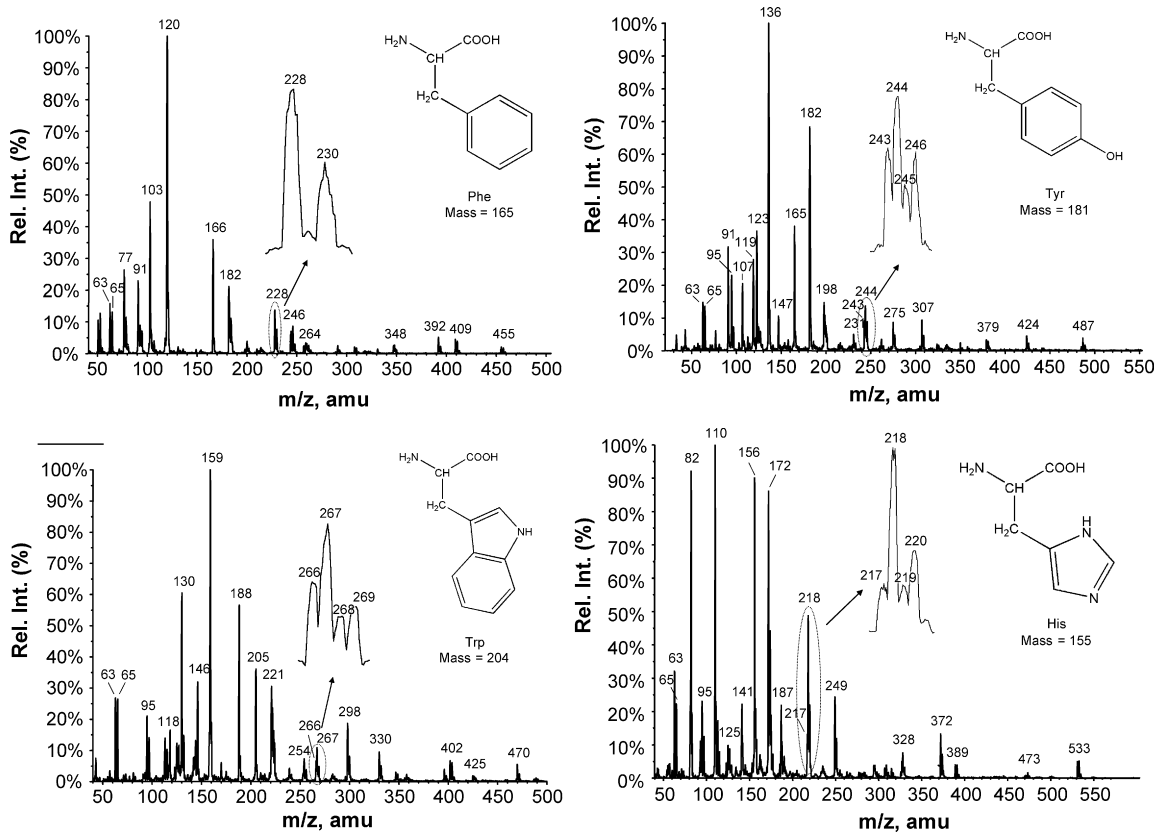

Fig. 1. ESI source spectra of the solutions of each aromatic amino acid and $CuSO_4$ in water/methanol 1:1 solvent.

hydrated complexes. The [Cu AA_{arom}]$^+$ complexes only appear at high values of DP. Fig. 1 shows the source spectra recorded at DP = 100 V (except for the case of *Phe* where DP = 110 V). The presence of the two isotopes of Cu (^{63}Cu and ^{65}Cu) leads to an easy identification of the Cu containing ions.

Low energy CID spectra of selected [Cu AA_{arom}]$^+$ complexes have been recorded at different collision energies. Several new ions are observed on the collision spectra of each amino acid. Fig. 2 shows the relative abundances of these ions in front of the collision energy. It can be observed that most of the fragmentations are common for all systems: loss of 46 u (CH_2O_2), which is always the most important fragmentation, loss of 61 u corresponding to the elimination of a fragment with CO_2NH_3 composition, likely consecutive elimination of NH_3 and CO_2 as proposed before for the [Ag Phe]$^+$ system, [32,33] and loss of 18 u corresponding to the elimination of H_2O. Two other peaks observed in the spectra are those at *m/z* 63 (Cu^+) and *m/z* 80 (NH_3Cu^+). It should be noted that in all cases the loss of $NH_3 + CO_2$ is a minor fragmentation of the complex except in the case of *His* where it is a major fragmentation channel.

The loss of 137 u to give R^+ is also observed in all cases, and different pathways could account for this elimination. Moreover, the presence of the peak corresponding to the loss of 108 u (elimination of CuCOOH to give the NH_2CHR^+ imonium ion) observed for the four cationized amino acids, suggests a possible consecutive elimination of CuCOOH and NH=CH_2 instead of a direct elimination of the $CuC_2O_2NH_4$ group.

The collision spectra also show the loss of 73 u corresponding to the elimination of a fragment with $C_2O_2NH_3$ composition. This elimination can be the result of the consecutive elimination of CH_2O_2 (the main fragmentation in all cases as noted above) and HCN or the direct elimination of $C_2O_2NH_3$. Calculations will help us to identify the most probable pathway for this and the other fragmentations.

It should be noted that at higher collision energies (not shown) only the peak corresponding to Cu^+ (*m/z* 63) rises in intensity. This is due to the fact that at high collision energies the decationization process is favored in front of other possible routes involving several energy barriers at higher internal energies, as pointed out by Hopilliard et al. for the case of [Cu Gly]$^+$ [27]. Therefore, the value of the binding energy of the [Cu AA_{arom}]$^+$ complexes is a good limit to distinguish which processes will be favorable.

Finally, based on the spectra of Fig. 1 one could think that the [Cu AA]$^+$ peaks of Tyr, Trp and His are contaminated by the isobaric ^{13}C satellites of the [Cu AA–H]$^+$ complexes, which contain Cu^{2+}. As a consequence, some of the fragments observed in the CID spectra could arise from these satellites. However, the examination of the CID spectra of the [Cu AA–H]$^+$ complexes have shown that the only peak with appreciable intensity shared by both types of complexes is that corresponding to the loss of 73 u for the case of His. Therefore the loss of 73 peak observed in the [Cu His]$^+$ CID spectrum of Fig. 2 can contain a small proportion of ions originated from the [Cu His-H]$^+$ complex.

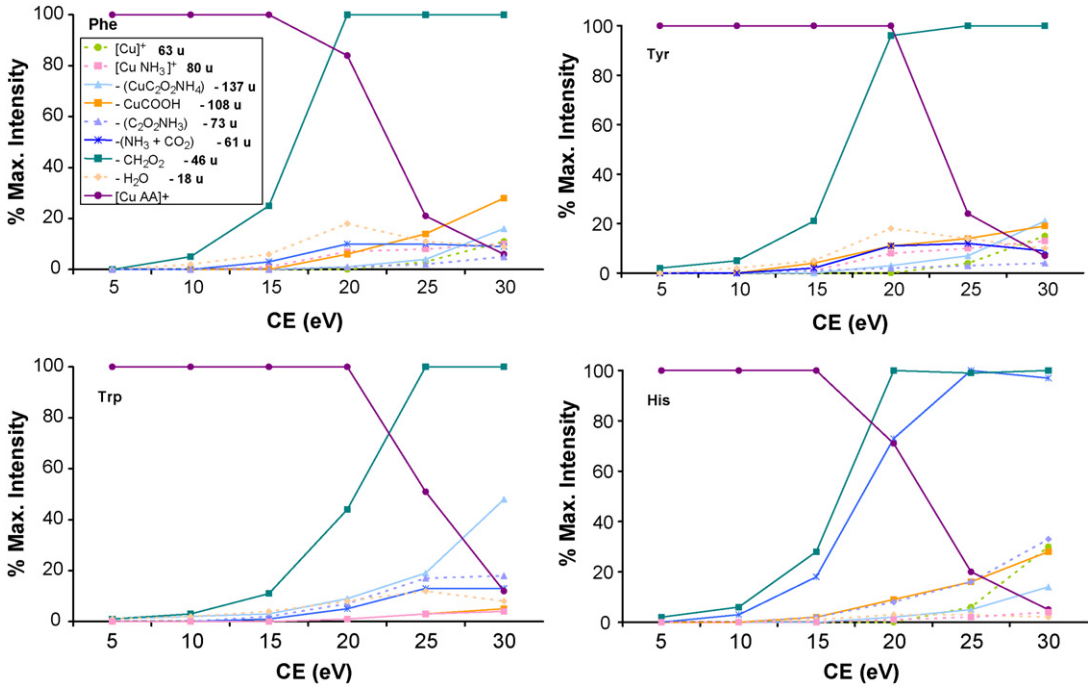

Fig. 2. Relative abundances of the observed ions after collisional activation of the corresponding parent $[Cu\ AA_{arom}]^+$ ion in front of the collision energy.

The observed losses are very similar for all the aromatic systems and only differ in their relative intensities. Consequently, it seems that losses do not involve the breaking of the side chain of the amino acid, in agreement with other previous metal cation–amino acid studies [32,33]. Therefore, we have selected only one of the considered systems, $[Cu\ Phe]^+$, for the study of its potential energy surface (including the ZPE corrections) by means of the B3LYP density functional method in order to rationalize the experimental findings.

4.1. Coordination of Cu^+ to Phe

The relative stability and structure of the different conformers of $[Cu\ Phe]^+$ have been considered. Among all the isomers found, three of them are separated by less than 4 kcal/mol. The geometries and relative potential energies with the ZPE of these isomers are shown in Fig. 3. The most stable structure corresponds to the metal cation interacting with the aromatic ring, the amine nitrogen and the carbonyl oxygen (**$PheCu^+$-1**). The other two structures correspond to the coordination of Cu^+ to the aromatic ring and the amine nitrogen (**$PheCu^+$-2**), and to the aromatic ring and the carbonyl oxygen (**$PheCu^+$-3**) of *Phe*. **$PheCu^+$-1** is similar to the most stable structure previously found for alkali-aromatic amino acids [47–56] systems; that is, the Cu^+ is bound by the NH_2, the CO and by the π system of the aromatic group. However, a significant difference can be observed: while for the alkaline systems the metal cations are centered above the aromatic ring, for Cu^+ the metal cation is interacting with the ring but coordinating only with the C–C bond, due to the ability of transition metal cations to efficiently reduce Pauli repulsion by sd and dp hybridization. Tricoordinated structures in which the metal cation interacts with the amino group, the carbonyl group and the side chains, have also been found for other Cu^+–amino acid systems such as serine and cysteine [57].

Structure **$PheCu^+$-1** has been taken as reference for the calculations of the different mechanisms. The interaction energy for this structure is 83.5 kcal/mol at the B3LYP level. This value will be taken as the limit to consider if a process is favorable or not.

Hereafter, the following nomenclature will be used to identify the different stationary points involved in the fragmentation mechanisms. Species formed through mechanisms involving

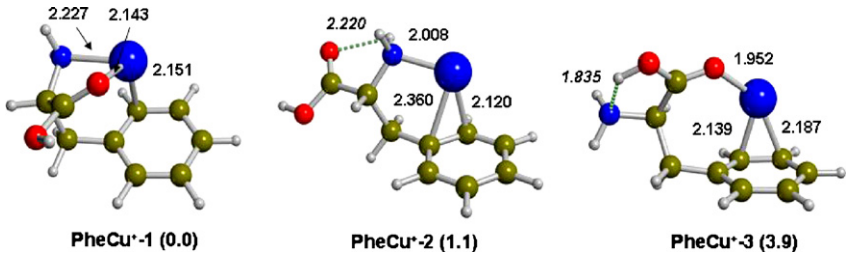

Fig. 3. B3LYP-optimized geometries for the most stable conformers of the $[Cu\ Phe]^+$ system. The relative energies are shown in parenthesis. Distances are in Å and energies in kcal/mol.

C_α-COOH insertion will be referred as CC*n* where *n* stands for the mass lost. That is, CC46 structures correspond to species involved in the loss of 46 via C–C insertion mechanism. Similarly, structures resulting from the metal insertion between C_α and the lateral chain will be referred as CR.

4.2. Loss of 46 u mechanisms

The composition associated with 46 u is CH_2O_2 and the corresponding ion resulting from this fragmentation is commonly observed both in cationized and protonated amino acids. In our case, this is the most important elimination and different mechanisms have been proposed in the literature that account for this fragmentation in cationized amino acids: loss of formic acid (HCOOH), consecutive loss of H_2O and CO or consecutive loss of CO_2 and H_2. It is generally accepted that the most probable mechanism involves the consecutive elimination of H_2O and CO [24,27]. Moreover, Hoppilliard et al. have shown that this mechanism is the less energetically demanding in the case of $[Cu\ Gly]^+$ [27]. On the other hand, elimination of CO_2 and H_2 has an activation barrier considerably higher than the other two channels. As a consequence, we have focused in the elimination of HCOOH and the elimination of $H_2O + CO$.

Insertion of the metal cation into the C–C or the C–OH bonds of the amino acid have been traditionally invoked as the initial steps of the mechanisms leading to the elimination of 46 u. We have investigated the C–C insertion but not the C–OH because the initial $[Cu\ Phe]^+$ structures do not seem to be suitable for such insertion. First, the structure that results upon complexation to the OH and NH_2 lays 16.4 kcal/mol above **PheCu$^+$-1** and does not involve coordination between the metal cation and the aromatic ring. Such a structure is similar to the analogous for the $[Cu\ Gly]^+$ complex and owing to that for this system the insertion to C–OH was found to be less favorable than the C–C one, we do not expect major changes for the present case. An additional non-insertion mechanism has been considered and is initiated by a hydrogen transfer from the amine to the OH group leading to the formation of H_2O.

Fig. 4 shows the mechanisms arising from the C–C metal cation insertion that lead to the elimination of 46 u. The insertion of Cu^+ into the C–C bond yields an intermediate (**CC46-1**) through the transition state **CC46-TS1**. The IRC calculation from this structure indicates that the transition state does not connect with any of the three most stable structures of $[Cu\ Phe]^+$ but with another isomer, **PheCu$^+$-4**, 8.4 kcal/mol higher in energy than the most stable one. Any attempt to locate a transition state for the C–C insertion connecting with the one of the most stable structures collapsed to the **CC46-TS1** structure. However, the interconversion barrier leading to **PheCu$^+$-4** (11.1 kcal/mol) is much lower than the other steps of the mechanisms, as shown in Fig. 4.

The intermediate **CC46-1** can evolve through two different pathways. The most energetic one (not shown) proceeds via a hydrogen transfer from the amine group to the carboxylic group through a transition structure whose energy barrier is 40.8 kcal/mol and producing an intermediate containing formic acid as a ligand. Detachment of formic acid leads to the loss of 46 u product, **CC46-6** located at 53.1 kcal/mol above **PheCu$^+$-1**. The second possible pathway proceeds via a hydrogen transfer from the amine group to the OH group of **CC46-1** resulting in the formation of **CC46-2**. This is a very stable tricoordinated complex where the metal cation is coordinated to CO, H_2O and to the aromatic ring. The fragmentation of **CC46-2** can produce the elimination of one or two of these ligands. Elimination of H_2O produces **CC46-3** (5.9 kcal/mol above **PheCu$^+$-1**), while elimination of CO leads to **CC46-5** being 22.8 kcal/mol above **PheCu$^+$-1**. It should be mentioned that in the cases of $[Cu\ Phe]^+$, $[Cu\ Tyr]^+$ and $[Cu\ Trp]^+$ an almost insignificant amount (its relative abundance is always inferior to 2%) of the loss of CO product is observed in the CID spectra (not shown in Fig. 2). Nevertheless, both fragmentation peaks, loss of CO and loss of H_2O disappear rapidly as the collision energy increases.

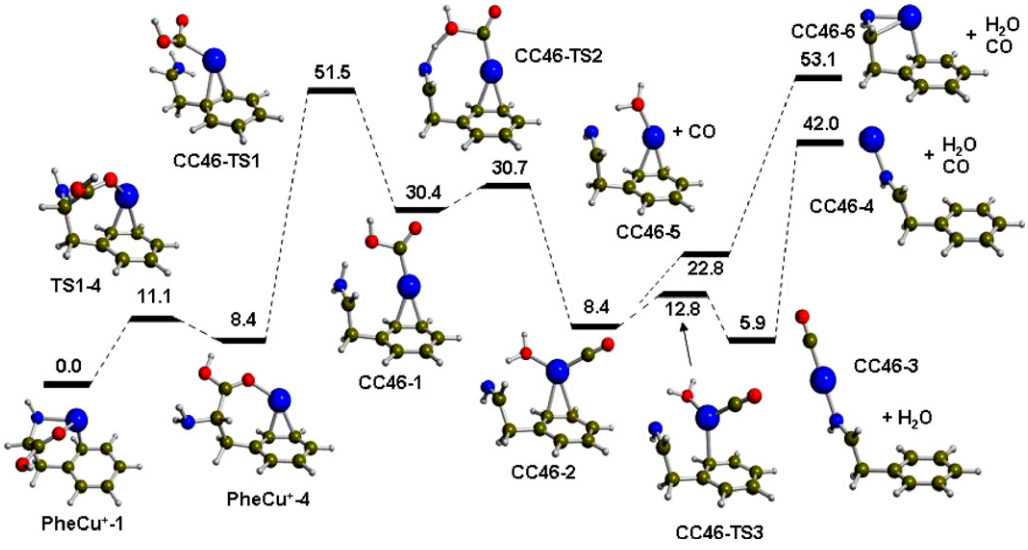

Fig. 4. Potential energy profile for the loss of 46 u starting with the Cu^+ insertion into the C–C bond.

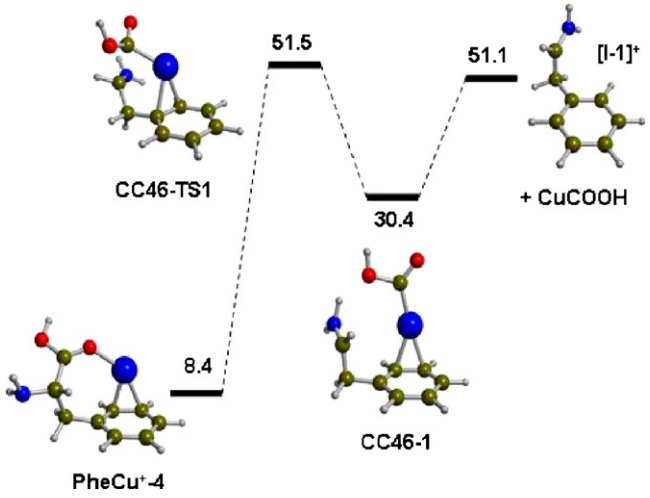

Fig. 5. Potential energy profile for the loss of 108 u.

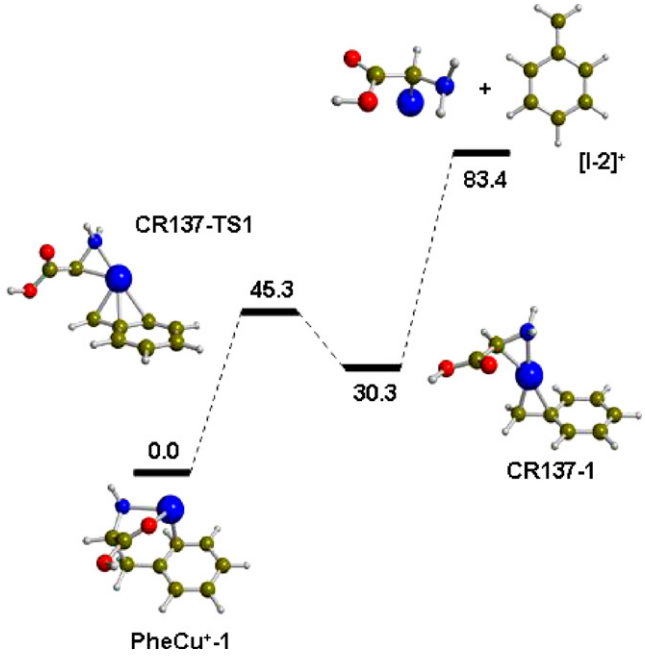

Fig. 6. Potential energy profile for the loss of 137 u.

Loss of CO from **CC46-3** leads to $Cu^+RCH{=}NH$ which is 42.0 kcal/mol higher in energy than **PheCu$^+$-1**. The limiting step of both mentioned pathways, elimination of HCOOH and consecutive elimination of H_2O and CO, is the metal cation insertion to produce **CC46-1** (51.5 kcal/mol) and therefore, the following steps after the insertion will have enough internal energy to decompose directly to the final products in agreement with the rapid extinction of the peaks corresponding to the loss or CO and loss of H_2O. Since the C–C insertion barrier is the highest one, both paths are energetically viable for the elimination of mass 46.

Elimination of C_2H_2O can also be achieved through another mechanism without any metal insertion. In this case a hydrogen transfer from the amine to the OH group of **PheCu$^+$-2** (after rotation of the C–COOH bond) leads to the direct elimination of H_2O and CO. The barrier for this fragmentation is 57.8 kcal/mol, significantly higher than those involved in the C–C insertion mechanism.

4.3. Loss of CuCOOH (108 u)—formation of the immonium ion NH_2CHR^+

The mechanism associated to the formation of the immonium ion is shown in Fig. 5 and starts with the insertion of the metal cation into the backbone C–C bond. This insertion leads to the **CC46-1** intermediate and direct elimination of CuCOOH from this structure leads to the immonium ion **[I-1]$^+$**. The energy barrier of the limiting step in this mechanism (51.5 kcal/mol) is the same that that of the loss of 46 u mechanism. However, Fig. 2 shows very different intensities for the peaks corresponding to these losses. This is probably due to the fact that for the loss of 108 the energy of the asymptote is of the same order than the C–C insertion barrier, in contrast to the loss of 46 for which the asymptote is much lower in energy.

4.4. Loss of 137 u

This fragmentation corresponds to the loss of a fragment with a $CuC_2O_2NH_4$ composition and two possibilities have been explored for this reaction. In the first case the consecutive elimination of CuCOOH and $NH{=}CH_2$ has been considered. Elimination of CuCOOH leads to the immonium ion, as commented above (**[I-1]$^+$** in Fig. 5), and the subsequent elimination of $NH{=}CH_2$ would lead to the loss of 137 u peak. The barrier for this last elimination is more than 140 kcal/mol from the **PheCu$^+$-1**, isomer showing that this pathway can be discarded. The second possibility (Fig. 6) is the direct elimination of $COOHCHNH_2Cu$. The path for this elimination starts with the insertion of the metal cation into the C–R bond leading to the **CR137-1** complex with an energy barrier of 45.3 kcal/mol. The decomposition of **CR137-1** directly leads to $COOHCHNH_2Cu$ + **[I-2]$^+$**. The energy of this asymptote is 83.4 kcal/mol above the most stable isomer, very similar to the binding energy of [Cu Phe]$^+$ (83.5 kcal/mol). It can be observed in Fig. 2 that both peaks, 63 u (Cu^+) and loss of 137 u appear at high collision energies (about 25 eV). In addition, it can also be observed that the intensity of this peak (loss of 137 u) is higher in the case of [Cu Trp]$^+$ than in the other amino acids. This is probably due to the presence of a second aromatic ring in the side chain of *Trp* that can delocalize more efficiently the positive charge located in the eliminated side chain **[I-2]$^+$**.

It should be noted that in the case of [Cu His]$^+$ the H_2OCu^+ complex also matches the loss of 137 peak. Formation of H_2OCu^+ can arise from the a tricoordinated complex similar to **CC46-2** (see Fig. 4) after losing the other two ligands, the energy of the final asymptote for this elimination being 70.6 kcal/mol. Therefore, this reaction channel cannot be completely discarded (the binding energy of [Cu His]$^+$ is 98.8 kcal/mol) and, indeed, the loss of 137 peak corresponds to a mixture of both complexes. Nevertheless, this is a minor peak in the His spectrum and the proportion corresponding to H_2OCu^+ is small as demonstrated by the absence of this peak in the spectra of the other amino acids.

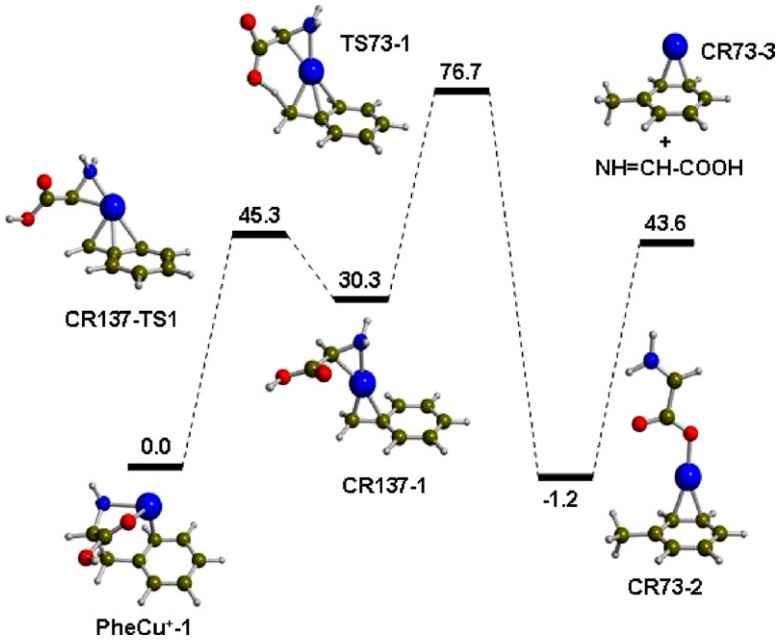

Fig. 7. Potential energy profile for the loss of 73 u.

4.5. Loss of 73 u ($C_2O_2NH_3$)

As in the previous case, this fragmentation can occur through two different ways. In the first case, the loss of $H_2O + CO$ could be followed by the elimination of HCN from **CC46-6** (see Fig. 4). The energy barriers associated to these mechanisms are always larger than 114 kcal/mol. Thus, the consecutive loss of H_2O, CO and HCN would not be a reasonable mechanism.

Another more probable way is the elimination of a $C_2O_2NH_3$ fragment as shown in Fig. 7. This elimination starts from the Cu^+ inserted intermediate **CR137-1** which could evolve through two different paths because two different hydrogen atoms can be transferred from the backbone of the amino acid to the CH_2 group of R, the hydrogen of the COOH group or one hydrogen atom of the NH_2 group. In the first case (shown in Fig. 7) the hydrogen transfer in **CR137-1** leads to a high stable complex, **CR73-2**, through a barrier of 76.7 kcal/mol. This is a complex where the cation is bound to the aromatic ring of R and to one oxygen of the CO_2CHNH_2 moiety. The direct decomposition of this complex would lead to **CR73-3** + $^+NH_2CHCO_2^-$ but such small zwitterionic structure is unstable in gas phase and very likely, while is being eliminated, simultaneous proton rearrangement occurs leading to **CR73-3** + NH=CH-COOH, the final products of this reaction path with a relative energy of 43.6 kcal/mol with regard to **PheCu$^+$-1**. In the second case, in order to facilitate the transfer of the hydrogen atom of the NH_2 group, a previous rotation of the Cu–CN bond should be produced. Unfortunately, all attempts of finding the transition state corresponding to this step have failed, and thus we assume that this process cannot proceed. However, the limiting step of the process calculated has a barrier of 76.7 kcal/mol, higher than the loss of 46 u mechanism, and therefore in agreement with the intensities of the spectra (Fig. 2).

4.6. Loss of 61 u

As commented previously, this loss must correspond to the elimination of NH_3 and CO_2. This elimination can be achieved through two different pathways. The first one is shown in Fig. 8 and starts with the metal cation insertion into the C–C bond of the zwitterionic structure **PheCu$^+$-zwit** leading to **CC61-1** with a barrier of 44.7 kcal/mol above the most stable conformer of [Cu Phe]$^+$ system. Consecutive elimination of CO_2 and NH_3 from **CC61-1** (not shown in Fig. 8) leads to an asymptote that is 59.8 kcal/mol above **PheCu$^+$-1,** higher than the barrier of the other possible route. The second pathway leads to **CC61-2** from **CC61-1** through a transition state, **CC61-TS2**, which is 36.8 kcal/mol above the most stable conformer. **CC61-2** can lose CO_2 without reverse activation barrier yielding **CC61-3** (15.3 kcal/mol less stable than **PheCu$^+$-1**). The opening of the three-member ring of **CC61-3** leads to **CC61-4** + CO_2 with an activation barrier of 8.6 kcal/mol respect to **CC61-3**. It should be noted that formation of **CC61-4** avoiding three-membered ring intermediates (**CC61-2** and **CC61-3**) is expected to be less favorable since it implies a 1,2-proton transfer. Fragmentation of **CC61-4** can take place through the elimination of NH_3 leading to **CC61-6** + CO_2 + NH_3 (26.8 kcal/mol higher than the energy of the ground state structure), or through the elimination of **CC61-5** leading to NH_3Cu^+ + **CC61-6** + CO_2, 1.5 kcal/mol more stable than the previous asymptote. Thus this would be the preferred elimination channel of this path. However, the step **CC61-1** → **CC61-2** through the **CC61-TS2** transition state implies a very important reorientation of the NH_3 and CO_2 moieties. The excess of internal energy into the system would favor the direct cleavage of the C–NH_3 bond in **CC61-TS2** leading to the direct elimination of NH_3. Further elimination of CO_2 yields **CC61-7** + CO_2 + NH_3, 59.8 kcal/mol higher in energy than the most stable complex. As a consequence, the limiting step in this

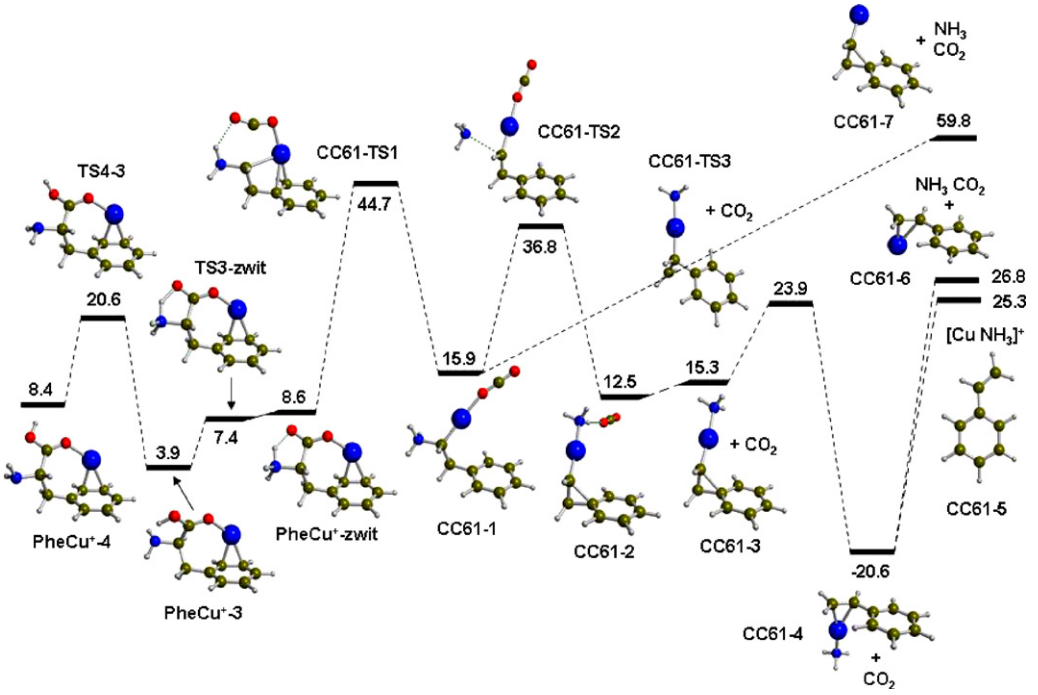

Fig. 8. Profile for the loss of 61 u starting with the Cu^+ insertion into the C—C bond.

mechanism has an energy barrier of 59.8 kcal/mol, much larger to that found in the case of the loss of 46 u, in agreement with the intensities found for both peaks in the CID spectra (see Fig. 2).

It is interesting to note that the peak corresponding to the elimination of $NH_3 + CO_2$ is always a minor fragmentation channel of the complexes except in the case of [Cu His]$^+$ where the intensity of that peak is very similar to the intensity of the loss of 46 u peak. The difference between *His* and the rest of the aromatic amino acids lies in the type of metal coordination. In the other three amino acids the most stable structure corresponds always to the metal cation interacting with the π system of the aromatic ring. However, in the case of *His* the metal cation coordinates to one nitrogen atom of the imidazole ring as shown in Fig. 9. The first conformer of [Cu His]$^+$ with the metal cation coordinated to the π system is around 20 kcal/mol above the most stable one. This different coordination of the metal cation in the case of *His* will probably induce differences in the reaction mechanisms for the observed fragmentations and therefore, differences in the observed intensities. For instance, preliminary calculations on the analogous **CC61-1** and **CC61-TS2** for the [Cu His]$^+$ complex show that the direct cleavage of the C–NH_3 bond is less favorable than CO_2 elimination since transition structures show C–N distances of 2.59 and 2.78 Å, for the [Cu His]$^+$ and [Cu Phe]$^+$ complexes, respectively. In this case, the barriers corresponding to the loss of CH_2O_2 and CO_2NH_3 are similar (44.1 and 46.5 kcal/mol, respectively) which would explain the similar intensities.

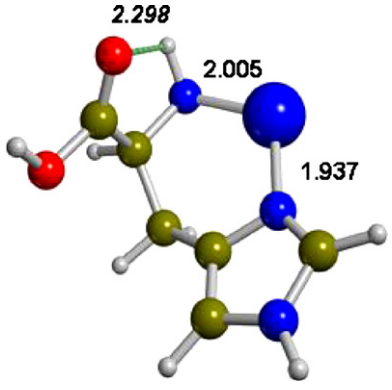

Fig. 9. B3LYP-optimized geometry for the most stable conformer of the [Cu His]$^+$ system. Distances are in Å.

Finally, it is worth noting that the fragmentation patterns observed in the ESI-CID spectra of [Cu AA_{arom}]$^+$ systems are similar to those observed for [Cu Gly]$^+$, that is, the most intense peak corresponds to the loss of H_2O and CO in all cases, and the main difference is that eliminations in which the side chain is implicated (loss of 73 and 137 u) and elimination of NH_3 and CO are not observed for [Cu gly]$^+$. Therefore, we can conclude that the side chain interaction has a minor influence on the fragmentation pattern of the aromatic amino acids. However, some peaks observed before in the ESI-CID spectrum of [Ag Phe]$^+$ do not appear in the spectra of [Cu AA_{arom}]$^+$ complexes showing that different metal cations can induce different reactivity of the aromatic amino acids.

5. Conclusions

The reactions of copper sulfate with aromatic amino acids in the electrospray source lead to the formation of [Cu AA_{arom}]$^+$ complexes at relatively high values of the declustering potential (DP). The collision-induced fragmentations of the metal cation complexes at different collision energies have been studied. All the aromatic amino acids show the same fragmentations,

the most important one being the loss of CH_2O_2 in all cases, as for glycine. Other fragmentations correspond to the loss of $CuC_2O_2NH_4$, CuCOOH, $C_2O_2NH_3$, CO_2NH_3, H_2O and formation of NH_3Cu^+. The dissociation of the complexes into Cu^+ and the respective amino acids is also observed in the spectra.

B3LYP calculations have been carried out for the [Cu Phe]$^+$ complex in order to rationalize the observed fragmentations. First, the structure of the [Cu Phe]$^+$ ion has been investigated and the most stable structure **PheCu$^+$-1** corresponds to the metal cation interacting with the nitrogen of the amino group, the carbonyl oxygen and the aromatic ring. The computed binding energy including the ZPE for this structure is 83.5 kcal/mol.

The exploration of the potential energy surface shows that most of the observed eliminations are produced from insertion of the metal cation into the backbone C–C bond of *Phe* (losses of CH_2O_2, CuCOOH, and CO_2NH_3) or into the C–R bond (losses of $CuC_2O_2NH_4$ and $C_2O_2NH_3$). The energy barriers of the different dissociation channels are in good agreement with the observed intensities in the CID spectrum of [Cu Phe]$^+$. Elimination of CH_2O_2 shows the lowest energy barrier in agreement with its larger intensity in the spectrum. For [Cu His]$^+$, loss of CO_2NH_3 presents similar intensity with loss of CH_2O_2 in contrast to the other aromatic amino acids due to the influence of N imidazole coordinating to the metal cation.

Acknowledgments

Financial support from DGICYT and DURSI, through the BQ2002-04112-C02-01 and SGR00182 projects, and the use of the Catalonia Supercomputer Center (CESCA) are gratefully acknowledged. A.R. is indebted to the Universitat Autònoma de Barcelona for a doctoral fellowship, and to the Université d'Evry-Val d'Essonne for the kind hospitality.

References

[1] R. Colton, A. D'Agostino, J.C. Traeger, Mass Spectrom. Rev. 14 (1995) 79.
[2] C.L. Gatlin, F. Turecek, in: R.B. Cole (Ed.), Electrospray Ionization Mass Spectrometry, John Wiley & Sons, Inc., New York, 1997.
[3] M.T. Rodgers, P.B. Armentrout, Acc. Chem. Res. 37 (2004) 989.
[4] K. Eller, H. Schwarz, Chem. Rev. 91 (1991) 1121.
[5] A. Fontijn (Ed.), Gas-Phase Metal Reactions, North-Holland, Amsterdam, 1992.
[6] B.S. Freiser (Ed.), Organometallic Ion Chemistry, Kluwer Academic Publishers, Dordrecht, 1995.
[7] M. Becchi, S. Rebuffat, J.Y. Dugast, S. Hlimi, B. Bodo, G. Molle, Rapid Commun. Mass Spectrom. 9 (1995) 37.
[8] S.W. Lee, H.S. Kim, J.L. Beauchamp, J. Am. Chem. Soc. 120 (1998) 3188.
[9] I.K. Chu, X. Guo, T.C. Lau, K.W.M. Siu, Anal. Chem. 71 (1999) 2364.
[10] I.K. Chu, T. Shoeib, X. Guo, C.F. Rodriquez, A.C. Hopkinson, K.W.M. Siu, T.C. Lau, J. Am. Soc. Mass Spectrom. 12 (2001) 163.
[11] I.K. Chu, D.M. Cox, X. Guo, I. Kireeva, T.-C. Lau, J.C. McDermott, K.W.M. Siu, Anal. Chem. 74 (2002) 2072.
[12] J.C. Ma, D.A. Dougherty, Chem. Rev. 97 (1997) 1303.
[13] D.A. Dougherty, Science 271 (1996) 163.
[14] P. Hudaky, A. Perczel, J. Phys. Chem. A 108 (2004) 6195.
[15] P. Deschamps, P.P. Kulkarni, B. Sarkar, Inorg. Chem. 43 (2004) 3338.
[16] J.J.R. Fraùsto da Silva, R.J.P. Williams (Eds.), The Inorganic Chemistry of Life, Clarendon Press, Oxford, 1991.
[17] B.A. Cerda, C. Wesdemiotis, J. Am. Chem. Soc. 117 (1995) 9734.
[18] D. Wen, T. Yalcin, A.G. Harrison, Rapid Commun. Mass Spectrom. 9 (1995) 1155.
[19] H. Lavanant, Y. Hoppilliard, J. Mass Spectrom. 32 (1997) 1037.
[20] H. Lavanant, E. Hecquet, Y. Hoppilliard, Int. J. Mass Spectrom. 185–187 (1999) 11.
[21] Q.P. Lei, I.J. Amster, J. Am. Soc. Mass Spectrom. 7 (1996) 722.
[22] S. Bouchonnet, Y. Hoppilliard, G. Ohanessian, J. Mass Spectrom. 30 (1995) 172.
[23] Y.D. Xu, X. Zhang, A.L. Yergey, J. Am. Soc. Mass Spectrom. 7 (1996) 25.
[24] M.J. Polce, S. Beranova, M.J. Nold, C. Wesdemiotis, J. Mass Spectrom. 31 (1996) 1073.
[25] B.A. Cerda, C. Wesdemiotis, Int. J. Mass Spectrom. 187 (1999) 107.
[26] M. Massaouti, M. Velegrakis, Int. J. Mass Spectrom. 225 (2003) 89.
[27] Y. Hoppilliard, G. Ohanessian, S. Bourcier, J. Phys. Chem. A 108 (2004) 9687.
[28] S.J. Lippard, J.M. Berg, Principles of Bioinorganic Chemistry, University Science Books, Mill Valley, CA, 1994.
[29] T. Yalcin, J. Wang, D. Wen, A.G. Harrison, J. Am. Soc. Mass Spectrom. 8 (1997) 749.
[30] L. Rodriguez-Santiago, M. Sodupe, J. Tortajada, J. Phys. Chem. A 105 (2001) 5340.
[31] L. Rodriguez-Santiago, M. Noguera, M. Sodupe, J.Y. Salpin, J. Tortajada, J. Phys. Chem. A 107 (2003) 9865.
[32] E.R. Talaty, B.A. Perera, A.L. Gallardo, J.M. Barr, M.J. Van Stipdonk, J. Phys. Chem. A 105 (2001) 8059.
[33] T. Shoeib, A.C. Hopkinson, K.W.M. Siu, J. Phys. Chem. B 105 (2001) 12399.
[34] A. Luna, B. Amekraz, J.P. Morizur, J. Tortajada, O. Mo, M. Yanez, J. Phys. Chem. A 101 (1997) 5931.
[35] A. Luna, B. Amekraz, J. Tortajada, J.P. Morizur, M. Alcami, O. Mo, M. Yanez, J. Am. Chem. Soc. 120 (1998) 5411.
[36] J. Bertrán, L. Rodriguez-Santiago, M. Sodupe, J. Phys. Chem. B 103 (1999) 2310.
[37] A. Luna, B. Amekraz, J.P. Morizur, J. Tortajada, O. Mo, M. Yanez, J. Phys. Chem. A 104 (2000) 3132.
[38] A.D. Becke, J. Chem. Phys. 98 (1993) 5648.
[39] C. Lee, W. Yang, R.G. Parr, Phys. Rev. B 37 (1988) 785.
[40] M.J. Frisch, G.W. Trucks, H.B. Schlegel, G.E. Scuseria, M.A. Robb, J.R. Cheesman, J.A. Montgomery, T. Vreven, K.N. Kudin, J.C. Burant, J.M. Millam, S.S. Iyengar, J. Tomasi, V. Barone, B. Mennucci, M. Cossi, G. Scalmanu, N. Rega, G.A. Petersson, H. Nakatsuji, M. Hada, M. Ehara, K. Toyota, R. Fukuda, J. Hasegawa, M. Ishida, T. Nakajima, Y. Honda, O. Kitao, H. Nakai, M. Klene, X. Li, J.E. Knox, H.P. Hratchian, J.B. Cross, C. Adamo, J. Jaramillo, R. Gomperts, R.E. Stratmann, O. Yazyev, A.J. Austin, R. Cammi, C. Pomelli, J.W. Ochterski, P.Y. Ayala, K. Morokuma, G.A. Voth, P. Salvador, J.J. Dannenberg, V.G. Zakrzewski, S. Dapprich, A.D. Daniels, M.C. Strain, O. Farkas, D.K. Malick, A.D. Rabuck, K. Raghavachari, J.B. Foresman, J.V. Ortiz, Q. Cui, A.G. Baboul, S. Clifford, J. Cioslowski, B.B. Stefanov, G. Liu, A. Liashenko, P. Piskorz, I. Komaromi, R.L. Martin, D.J. Fox, T. Keith, M.A. Al-Laham, C.Y. Peng, A. Nanayakkara, M. Challacombe, P.M.W. Gill, B. Johnson, W. Chen, M.W. Wong, C. Gonzalez, J.A. Pople, Gaussian 03, Gaussian Inc., Wallingford, CT, 2004.
[41] C.W. Bauschlicher, A. Ricca, H. Partridge, S.R. Langhoff, Recent Advances in Density Functional Theory, Part II, World Scientific Publishing Co., Singapore, 1997.
[42] W. Koch, M.C. Holthausen, A Chemists's Guide to Density Functional Theory, WILEY-VCH Verlag, Weinheim, Federal Republic of Germany, 2001.
[43] A. Luna, M. Alcamí, O. Mó, M. Yáñez, Chem. Phys. Lett. 320 (2000) 129.
[44] A.J.H. Wachters, J. Chem. Phys. 52 (1970) 1033.
[45] P.J. Hay, J. Chem. Phys. 66 (1977) 4377.
[46] K. Raghavachari, G.W. Trucks, J. Chem. Phys. 91 (1989) 1062.
[47] F.M. Siu, N.L. Ma, C.W. Tsang, Chem. Eur. J. 10 (2004) 1966.
[48] V. Ryzhov, R.C. Dunbar, J. Am. Chem. Soc. 121 (1999) 2259.
[49] R.C. Dunbar, J. Phys. Chem. A 104 (2000) 8067.
[50] A. Gapeev, R.C. Dunbar, J. Am. Chem. Soc. 123 (2001) 8360.
[51] F.M. Siu, N.L. Ma, C.W. Tsang, J. Am. Chem. Soc. 123 (2001) 3397.

[52] A. Gapeev, R.C. Dunbar, Int. J. Mass Spectrom. 228 (2003) 825.
[53] M.M. Kish, G. Ohanessian, C. Wesdemiotis, Int. J. Mass Spectrom. 227 (2003) 509.
[54] C. Ruan, M.T. Rodgers, J. Am. Chem. Soc. 126 (2004) 14600.
[55] N.C. Polfer, B. Paizs, L.C. Snoek, I. Compagnon, S. Suhai, G. Meijer, G. Von Helden, J. Oomens, J. Am. Chem. Soc. 127 (2005) 8571.
[56] A.S. Reddy, G.N. Sastry, J. Phys. Chem. A 109 (2005) 8893.
[57] S. Hoyau, G. Ohanessian, J. Am. Chem. Soc. 119 (1997) 2016.